



Mechanism of Neutrophil p90RSK-Nrf2 Signaling Pathway in Atherosclerosis

Jiawen Li¹, Lei Wang¹, Xiao Liang², Xiaoxia Li³

¹Department of Cardiology, The Fourth Affiliated Hospital of Harbin Medical University, Harbin, China

²Department of Cardiology, The First Affiliated Hospital of Harbin Medical University, Harbin, China

³Department of Medical Laboratory, The Fourth Affiliated Hospital of Harbin Medical University, Harbin, China

Background: MRP8/14, a calcium-binding protein of the S100 family, is predominantly expressed in myeloid cells and exhibits proinflammatory and prothrombotic properties. Platelet-neutrophil interactions can trigger MRP8/14 release, but their role in atherosclerosis (AS) remains unclear.

Aims: To investigate the effect of MRP8/14 on AS progression and the underlying mechanisms involved, focusing on neutrophil activation and the toll-like receptor 4 (TLR4)-ERK1/2-p90RSK and NRF2-ARE pathways.

Study Design: Ex vivo and animal study.

Methods: Neutrophils isolated from mouse bone marrow were stimulated with P-selectin to induce MRP8/14 release, which was subsequently quantified using ELISA. Neutrophil extracellular traps (NET) formation was induced by phorbol 12-myristate 13-acetate, and Mrp8/14 expression was examined via fluorescence labeling. Cytokine release and CD11b

expression were assessed using flow cytometry. An AS mouse model was established by administering a high-fat diet. Atherosclerotic plaque size was analyzed using Oil Red O staining. Proteins from the TLR4-ERK1/2-p90RSK and NRF2-ARE pathways were analyzed by Western blotting.

Results: P-selectin induced MRP8/14 release, which was inhibited by P-selectin antagonists. NET formation also contributed to MRP8/14 secretion. hMRP8/14 treatment enhanced CD11b expression, neutrophil adhesion, and proinflammatory cytokine secretion. In AS mice, MRP8/14 secretion was linked to TLR4 upregulation, ERK1/2-p90RSK signaling activation, and NRF2-ARE pathway inhibition. Paquinimod, an MRP8/14 antagonist, mitigated neutrophil activation, inflammation, and arterial plaque formation.

Conclusion: MRP8/14 secreted from neutrophils activates the ERK1/2-p90RSK pathway via TLR4 and suppresses the NRF2-ARE pathway, driving inflammation and promoting AS progression.

INTRODUCTION

Atherosclerosis (AS) is a systemic vascular disease characterized by increased arterial intima-media thickness, atherosclerotic plaque formation, and sustained arterial stiffness. Its development is driven by risk factors such as diabetes mellitus, hypertension, and cigarette smoking, as well as genetic and environmental influences.^{1,2} Most cardiovascular diseases, including myocardial infarction, stroke, and sudden death, are attributable to AS plaque rupture.^{3,4} According to statistics, the global incidence of AS-related peripheral arterial disease steadily increased from 1990 to 2019, with approximately 113 million patients aged 40 and above affected in 2019. The

incidence rate also showed a positive correlation with advancing age.⁵ Currently, China has over 200 million individuals aged 65 and older, representing approximately 14.2% of the entire population. This demographic shift has resulted in a significant increase in the prevalence of AS-related diseases (including ischemic stroke, peripheral arterial disease, and ischemic heart disease).^{6,7} Therefore, AS has emerged as a global health concern, underscoring the importance of investigating its pathophysiological mechanisms and identifying potential therapeutic targets for intervention.

The pathogenesis of AS is a prominent focus of contemporary medical research. AS lesions initiate with endothelial dysfunction, which



Corresponding author: Xiao Liang, Department of Cardiology, The First Affiliated Hospital of Harbin Medical University, Harbin, China

e-mail: xiaoliang_hmu@163.com

Corresponding author: Xiaoxia Li, Department of Medical Laboratory, The Fourth Affiliated Hospital of Harbin Medical University, Harbin, China

e-mail: LJW96546LLL@hotmail.com

Received: April 23, 2025 **Accepted:** June 10, 2025 **Available Online Date:** 01.07.2025 • **DOI:** 10.4274/balkanmedj.galenos.2025.2025-4-73

Available at www.balkanmedicaljournal.org

ORCID iDs of the authors: J.L. 0000-0003-3959-0637; L.W. 0009-0005-3570-7035; X.L. 0009-0003-9862-3520; X.Li. 0009-0001-3546-2673.

Cite this article as: Li J, Wang L, Liang X, Li X. Mechanism of Neutrophil p90RSK-Nrf2 Signaling Pathway in Atherosclerosis. Balkan Med J; 2025; 42(4):347-57.

Copyright@Author(s) - Available online at <http://balkanmedicaljournal.org/>

promotes monocyte recruitment and triggers an inflammatory response, resulting in smooth muscle proliferation, foam cell formation, and the development of fatty streaks.^{8,9} Chronic immune mechanisms in the vascular wall significantly contribute to AS development.^{10,11} Studies have shown that inflammatory markers in the peripheral blood of AS patients are elevated compared to the general population. This process is linked to platelet-neutrophil interactions, with aberrant neutrophil recruitment playing a key role in sustaining chronic inflammation.^{12,13} MRP8/14, also known as S100A8/A9, belongs to the calcium-binding S100 family of proteins, which are expressed primarily in myeloid cells and have proinflammatory and prothrombotic properties.^{14,15} MRP8/14 comprises 40% of the cytoplasmic protein content of neutrophils and is secreted during the inflammatory response. MRP8/14 binds to toll-like receptor 4 (TLR4) in platelets and further promotes neutrophil recruitment and the inflammatory response.¹⁶ However, the impact of MRP8/14 on AS progression and its underlying mechanisms remains poorly understood.

The activation of inflammation-related signaling pathways is crucial in AS progression. Interleukin (IL)-8-induced neutrophil extracellular traps (NETs) exacerbate AS pathology progression by activating the NF- κ B pathway in macrophages.¹⁷ As a member of the transmembrane signaling receptor family that mediates innate immunity, TLR4 initiates the synthesis of various proinflammatory factors and chemokines upon binding to ligands such as lipopolysaccharides (LPS) and teichoic acid, which are involved in various aspects of AS initiation, progression, and plaque rupture.^{18,19} Singh et al.²⁰ revealed that oxidative stress induces p90RSK phosphorylation, mediates ERK5 S496 phosphorylation, and inhibits the Nrf2-ARE signaling pathway, thereby inducing an inflammatory response and promoting AS progression. In addition, the extracellular signal-regulated kinase (ERK) pathway is a key regulator of AS inflammation. Upon activation, phosphorylated ERK1/2 translocates from the cytoplasm to the nucleus and triggers transcription by phosphorylating p90RSK.²¹ Notably, TLR4 activates the ERK1/2 signaling pathway in vascular endothelial cells, contributing to abnormal angiogenesis.²²

Given that MRP8/14 primarily functions by binding to TLR4, and based on previous studies along with recent advances in domestic and international research, we hypothesized that MRP8/14 activates the ERK1/2-p90RSK signaling pathway by binding to TLR4, thereby inhibiting the Nrf2-ARE signaling pathway and amplifying inflammatory responses. Therefore, in this study, we isolated neutrophils from mouse bone marrow to examine the relationship between MRP8/14 secretion, neutrophil activation, and NET formation and to investigate the regulatory effects of MRP8/14 on the ERK1/2-p90RSK pathway and the Nrf2-ARE pathway. In addition, an AS mouse model was established using a high-fat diet (HFD) to explore the *in vivo* effects of MRP8/14 on AS progression. The objective of this research was to explore the effect and mechanism of action of MRP8/14 on the progression of AS and to identify novel therapeutic targets for AS treatment.

MATERIALS AND METHODS

Neutrophil isolation and processing

Male C57BL/6 mice (16–19 g, 6 weeks old) were procured from Vitalriver (Beijing, China). In accordance with the method outlined in a previous study¹², the mice were anesthetized and subsequently euthanized. Then, the tibia and femur were separated, and the surrounding residual muscle tissue was excised. The bone ends were severed using sterile surgical scissors, and the bone marrow was thoroughly rinsed with precooled phosphate-buffered saline (PBS) until the marrow cavity appeared white. The collected bone marrow cell suspension was centrifuged for 5 minutes (min), and the precipitated cell mass was resuspended in 1 mL of PBS after discarding the supernatant. Percoll solution [P4937, Sigma-Aldrich, St. Louis, MO, United States of America (USA)] at concentrations of 72%, 64%, and 54% was added to the centrifuge tube, and 1 mL of the bone marrow monocyte suspension was added to the top layer. Following centrifugation, the dense cell layer at the interface between the 64% and 72% Percoll isolate layers was carefully collected and rinsed three times with PBS to remove any residual Percoll solution. The isolated neutrophils were transferred to RPMI 1640 culture medium (12633020, Gibco, Grand Island, NY, USA) supplemented with 1% penicillin and streptomycin (15140122, Gibco) and incubated at 37 °C with 5% CO₂.

The isolated neutrophils were treated with PBS or 100 ng/mL of P-selectin (ADP3-050, R&D Systems, Minneapolis, MN) for 10 or 30 min. The neutrophils in the P-selectin + pneumonia severity index (PSI)-697 group were exposed to P-selectin (100 ng/mL) and PSI-697 (200 μM, HY-15526, MedChemExpress, Monmouth Junction, NJ, USA) for 10 min.²³ As described in a previous study¹², neutrophils were treated with LPS (1 μg/mL, L861706, Macklin, Shanghai, China) or human MRP8/14 protein [human recombinant MRP8/14 (hMRP8/14), 1.5 mg/mL, HY-P71076, MedChemExpress] for 30 min to induce neutrophil activation. The hMRP8/14 + paquinimod group was treated with paquinimod (100 μmol/L, HY-100442, MedChemExpress) for 4 h after the hMRP8/14 treatment for 30 min. In the LPS + paquinimod group, neutrophils were treated with LPS for 30 min, followed by paquinimod treatment for 4 h. In signaling pathway probing, neutrophils were initially treated with hMRP8/14 for 30 min, followed by a 4-hour exposure to one of the following: the p90RSK inhibitor FMK-MEA (10 μM, HY-52101C, MedChemExpress)²⁴, the p90RSK agonist Ceramide C6 (10 μM, HY-19542, MedChemExpress)²⁵, the ERK5-specific inhibitor AX15836 (5 μM, HY-101846, MedChemExpress)²⁶, the ERK5 agonist epidermal growth factor (EGF, 50 ng/mL, HY-P70590, MedChemExpress)²⁷, the Nrf2 inhibitor ML385 (1 μM, HY-100523, MedChemExpress)²⁸, or the Nrf2 agonist CDDO-ME (1 μM, HY-14909, MedChemExpress).²⁹

MRP8/14 level measurement

The MRP8/14 levels in neutrophil supernatants were evaluated utilizing the Mouse MRP8/14 (S100A8/S100A9) ELISA Kit (ab267630, Abcam, Cambridge, MA, USA). Neutrophils subjected to different treatments were centrifuged, and the resultant supernatant was

added to ELISA plates pre-coated with an MRP8/14-specific antibody and incubated for 2.5 h. After three washes with PBS, 100 µL of biotin-labeled antibody was introduced into each well and incubated at 37 °C for one hour. After discarding the liquid in the wells and washing three times with washing buffer, 100 µL of horseradish peroxidase-labeled streptavidin was added to each well, gently shaken, mixed, and incubated for 45 min. After washing with PBS, TMB substrate was applied according to the manufacturer's instructions and incubated for 30 min, avoiding light exposure. Following incubation, 50 µL of termination solution was added and mixed immediately. Then, the OD₄₅₀ value was measured, and the concentration was calculated. Furthermore, following the method outlined by Schenten et al.³⁰, neutrophils were exposed to diphenyleneiodonium (DPI, 10 µM, D2926, Sigma-Aldrich) for 30 min to inhibit reactive oxygen species (ROS) generation. The cells were subsequently exposed to phorbol 12-myristate 13-acetate (PMA, 100 nM, HY-18739, MedChemExpress) for 6 h. The concentration of MRP8/14 in the cell supernatant was then determined according to the procedure described above.

NET formation assay

As outlined by Sprenkeler et al.³¹, neutrophils were inoculated into 12-well plates and exposed to PMA at 37 °C for 4 h to induce NET formation. The cells were then treated with 4% paraformaldehyde (441244, Sigma-Aldrich) for 20 min at room temperature and blocked with 5% bovine serum albumin (BSA, V900933, Sigma-Aldrich) for 30 min. We added MRP8/14 primary antibody (ab288715, 1:500, Abcam) or elastase primary antibody (ELA, ab21590, 1:100, Abcam) dropwise to the cell surface and left it to incubate for 1 h at 37 °C protected from light exposure. Next, the secondary goat anti-rabbit IgG antibody (ab7171, 1:1000, Abcam) was applied and incubated for 1 h at 37 °C in the dark. Additionally, DNA was stained with Hoechst 33342 staining solution (C1028, Beyotime, Shanghai, China).³⁰ The samples were observed using a fluorescence microscope (EVOS, Thermo Fisher Scientific, Waltham, MA, USA), and the fluorescence levels were quantified using ImageJ software (version 1.54h, Wayne Resband, National Institute of Mental Health, USA).

Neutrophil activation marker assay

Following the respective treatments, the neutrophils were rinsed once with sterile PBS and resuspended to prepare a single-cell suspension (1.0×10^7 /mL). The cell suspension was mixed well with FITC-labeled CD11b antibody (11-0112-82, Invitrogen, Carlsbad, CA, USA) and incubated for 30 min in the dark. Cell activation was observed via flow cytometry (BD FACSCalibur™, BD Biosciences, San Jose, CA, USA), and the experimental findings were analyzed using FlowJo software (v10.8, BD Biosciences).

Calcein AM staining

Neutrophil activation was assessed using a Calcein AM fluorescent probe (C2012, Beyotime), following the method described by Sprenkeler et al.³¹ Neutrophils were inoculated into 96-well plates and following respective treatments, the supernatant was discarded. Calcein AM Staining Workup (1 µM) was added to achieve a cell density of 1×10^6 /mL. After incubation at 37 °C for 30 min, the cells were rinsed three times with PBS. Subsequently, the cells were

lysed using 0.5% Triton X-100 (T6328, Macklin), and the fluorescence level was quantified through a microplate reader (Infinite F200 PRO, Tecan, Männedorf, Switzerland). The percentage of adherent cells was calculated as follows: adherent cells % = number of Calcein AM-labeled cells/total cells × 100%.

Neutrophils trigger assay

The release of H₂O₂ was measured using the Amplex Red hydrogen peroxide (H₂O₂) kit (A22188, Invitrogen) following the protocol described by Sprenkeler et al.³¹ Neutrophils were inoculated into 96-well plates and exposed to PBS, LPS, or hMRP8/14 for 30 min before stimulation with fMLF (1 µM, F3506, Sigma-Aldrich) to trigger ROS production. Following the guidelines of the kit, the release of H₂O₂ was quantified, and fluorescence levels were measured using a microplate reader.

In vivo experiments

Male apolipoprotein E knockout (ApoE-/-) mice (20 ± 22 g, 6 weeks old) were acquired from Vitalriver (Beijing, China). The mice were placed in an SPF-grade animal holding room for one week of acclimatization. The rearing temperature was 22–24 °C, with a relative humidity of 55% to 60%, a 12-hour light-dark cycle, and the room was well ventilated. All mice were provided ad libitum access to food and water throughout the study period.

Based on the method outlined in a previous study¹², the mice were randomly assigned to four different groups: control (normal diet), HFD, paquinimod, and HFD + paquinimod (n = 6). The mice in the HFD group were fed with a HFD (TP23301, Trophic Animal Feed High-tech Co. Ltd., Nantong, Jiangsu, China) to establish an AS model. Mice in the Paquinimod group were orally administered drinking water containing paquinimod (25 mg/kg/d) daily. In the HFD + paquinimod group, paquinimod was administered orally daily, followed by HFD feeding. After 12 weeks, plasma samples were collected, and the mice were euthanized using sodium pentobarbital (100 mg/kg). Intact aortas were then dissected and isolated for further experiments. Approval for the animal research was obtained from the Animal Ethics and Welfare Committee.

Oil Red O staining

Mouse aortic tissues were fixed in 4% paraformaldehyde at 4 °C overnight. On the subsequent day, aortic tissues were incubated with Oil Red O stain (O0625, Sigma-Aldrich) for half an hour and rinsed with PBS solution. The sample was immersed in 60% isopropanol solution (563935, Sigma-Aldrich) for 1 min, followed by a two-minute rinse with distilled water. The samples were examined and photographed using a microscope (XK-DZ004, SINICO Optical Instrument Co., LTD, Shenzhen, China), and the area of the AS plaques was quantified using ImageJ software.

Immunofluorescence

Neutrophils were seeded at a density of 50%-60% in 12-well plates and fixed with 4% paraformaldehyde for 20 min. Mouse aortic tissues were exposed to 4% paraformaldehyde for 24 h, dehydrated through a graded ethanol series, embedded in paraffin, and sectioned

into 4-5 μm slices. The sections were deparaffinized using xylene (X821391, Macklin), rehydrated through gradient ethanol exposure, followed by antigen repair. The cell surface and tissue sections were permeabilized with 0.3% Triton X-100 for 10 min, followed by blocking with 5% BSA for 30 min. Next, cells were incubated with citrullinated histone h3 (CitH3) primary antibody (97272S, 1:300, Cell Signaling Technology, Danvers, MA, USA), MRP8/14 primary antibody (1:100, 6279-RBM5-P1, Invitrogen, Inc. Carlsbad, CA, USA), or myeloperoxidase (MPO) primary antibody (1:100, ab208670, Abcam) at 4 °C overnight. On the second day, cells were incubated with FITC-labeled goat anti-rabbit IgG (1:100, F-2765, Invitrogen) for 1 h at 37 °C in the dark. Subsequently, DAPI staining solution (C1005, Beyotime) was added and incubated for 10 min in the dark. Fluorescence signals were observed using a fluorescence microscope and analyzed with ImageJ software.

ELISA

IL-17 (ml037866), IL-22 (ml063138), tumor necrosis factor alpha [Tumor necrosis factor alpha (TNF- α), ml002095], IL-6 (ml098430), interferon-gamma (IFN- γ , ml002277), IL-8 (ml058632), and IL-10 (ml037873) ELISA Kits were procured from Enzyme-linked Biotechnology (Shanghai, China). As previously mentioned, ELISA kits were used to measure the cytokine content in neutrophil supernatants.

Mouse plasma was collected, and plasma levels of total cholesterol (TC, ml037202, Enzyme-linked Biotechnology), triglycerides (TG, CB10296, COIBO Bio, Shanghai, China), low-density lipoprotein cholesterol [low density lipoprotein cholesterol (LDL-C) CB10260, COIBO Bio], and high-density lipoprotein cholesterol (HDL-C, CB10316, COIBO Bio) were measured using ELISA kits. In addition, MRP8/14, IL-1 β (ml106733), TNF- α , IL-17, IL-6, and IL-22 levels in mouse serum were quantified using ELISA kits.

Western blot analysis

RIPA lysis buffer (P0013B, Beyotime) was added to neutrophil or mouse aortic tissue, and the resulting lysates were collected for protein extraction. The protein content was assayed using a BCA protein concentration assay kit (P0012, Beyotime). Following protein separation using SDS-PAGE (12%, WBT41220BOX, Invitrogen), the samples were moved to a PVDF membrane (88585, Invitrogen), which was sealed for three hours with 5% BSA. After membrane washing, the cells were incubated overnight at 4 °C with the following primary antibodies: TLR4 primary antibody (1:200, 48-2300, Invitrogen), ERK1/2 primary antibody (1:1000, MA5-15134, Invitrogen), p-ERK1/2 primary antibody (1:1000, MA5-38228, Invitrogen), p90RSK primary antibody (1:5000, PA5-29215, Invitrogen), p-p90RSK primary antibody (1:1000, AR865, Beyotime), ERK5 S496 primary antibody (1:1000, PA5-17689, Invitrogen), Nrf2 primary antibody (1:500, PA5-27882, Invitrogen), p-ERK5 S496 primary antibody (1:1000, 44-612G, Abcam), HO-1 primary antibody (1:1000, PA5-77833, Invitrogen), or NAD(P)H: quinone oxidoreductase 1 (NQO1) primary antibody (1:1000, PA5-82294, Invitrogen). The following day, after three washes, the membrane was incubated with goat anti-rabbit secondary IgG (1:10000, 31460, Invitrogen) for 2 h at room temperature. Gel imaging equipment

(iBright CL1500, Thermo Fisher Scientific) was used to scan the membrane after the chemiluminescent agent ECL (HY-K1005, MedChemExpress) was evenly dripped onto it. Gray value analysis was conducted using ImageJ software, and the relative expression of protein was calculated as the ratio of its gray value to GAPDH (1:1000, PA1-987, Invitrogen).

Statistical analysis

At least three repetitions of each set of experiments were conducted. Statistical analysis was performed using the SPSS 26.0 software (IBM SPSS Statistics 26). The data of this experiment conformed to normal distribution and are expressed as mean \pm standard deviation. The Shapiro-Wilk test was performed to confirm the normality of the data, and Levene's test was employed to examine variance alignment. If the data were normal and homogeneous in variance, a one-way analysis of variance was employed to test for overall differences across the multiple groups, followed by Dunnett's test for pairwise comparisons. If the data do not meet the assumptions of normality or homogeneity of variance, the Kruskal-Wallis test was used, followed by pairwise comparisons using Dunn's test with Bonferroni correction. Statistical significance was established for group differences when $p < 0.05$. For plotting, the Prism software (Graphpad 9.0) was used.

RESULTS

The engagement of neutrophils with P-selectin induces MRP8/14 secretion

P-selectin, a key adhesion molecule expressed on the platelet surface, facilitates neutrophil recruitment and triggers an inflammatory response in the vessel wall, thereby accelerating AS progression.^{32,33} MRP8/14 levels in the supernatant of neutrophil culture were markedly elevated after 10 or 30 min of P-selectin treatment, indicating that the interaction of neutrophils with P-selectin causes MRP8/14 secretion (Figures 1a, b). PMA is frequently employed to induce NET formation.³¹ MRP8/14 levels in the supernatant significantly increased following PMA stimulation, with P-selectin treatment for 10 minutes inducing a comparable elevation. We discovered that treatment with the P-selectin antagonist PSI-697 for 10 min decreased MRP8/14 secretion from neutrophils, further confirming that P-selectin interacts with neutrophils to induce MRP8/14 release (Figure 1c).

MRP8/14 release is accompanied by NET formation and neutrophil activation

Next, we stimulated neutrophils with PMA to induce NET formation. Significant MRP8/14 fluorescence was observed by Hoechst, ELA, and MRP8/14 staining, suggesting a potential association between MRP8/14 release and NET formation (Figure 2a). ROS production is a key indicator of PMA-induced NET formation.³⁰ To investigate the relationship between NET formation and MRP8/14 release, we inhibited ROS production by treating neutrophils with DPI to inhibit NADPH oxidase activation. The findings indicated a significant increase in MRP8/14 secretion following 6 h of PMA treatment alone (Figure 2b). However, the release of MRP8/14 was significantly

decreased when neutrophils were treated with DPI for 30 minutes and PMA for 6 hours. This further confirmed that MRP8/14 release is associated with NET formation. Flow cytometry revealed that the levels of CD11b, an indicator of neutrophil activation, were markedly elevated after LPS treatment, whereas hMRP8/14 treatment also induced an elevation in CD11b levels, suggesting that MRP8/14 release induces neutrophil activation (Figures 2c, d). Adhesion is a crucial neutrophil function. Calcein AM staining revealed that both LPS and hMRP8/14 treatment significantly increased the percentage of neutrophil-adherent cells (Figure 2e). Neutrophils transition from a basal to an activated state in response to cytokines or chemokines-a process known as triggering.³⁴ H₂O₂ release is frequently employed to assess neutrophil triggering. We observed that both LPS and hMRP8/14 treatment resulted in a significant increase in neutrophil H₂O₂ release, suggesting that MRP8/14 can mediate neutrophil triggering (Figure 2f). Furthermore, LPS or hMRP8/14 treatment significantly increased proinflammatory cytokines (IL-17, IL-22, IL-8, IFN-γ, TNF-α, IL-6) and reduced the anti-inflammatory cytokine IL-10 in neutrophil supernatants, confirming that MRP8/14 secretion promotes neutrophil activation and inflammatory responses (Figures 2g-m, Supplementary Table 1).

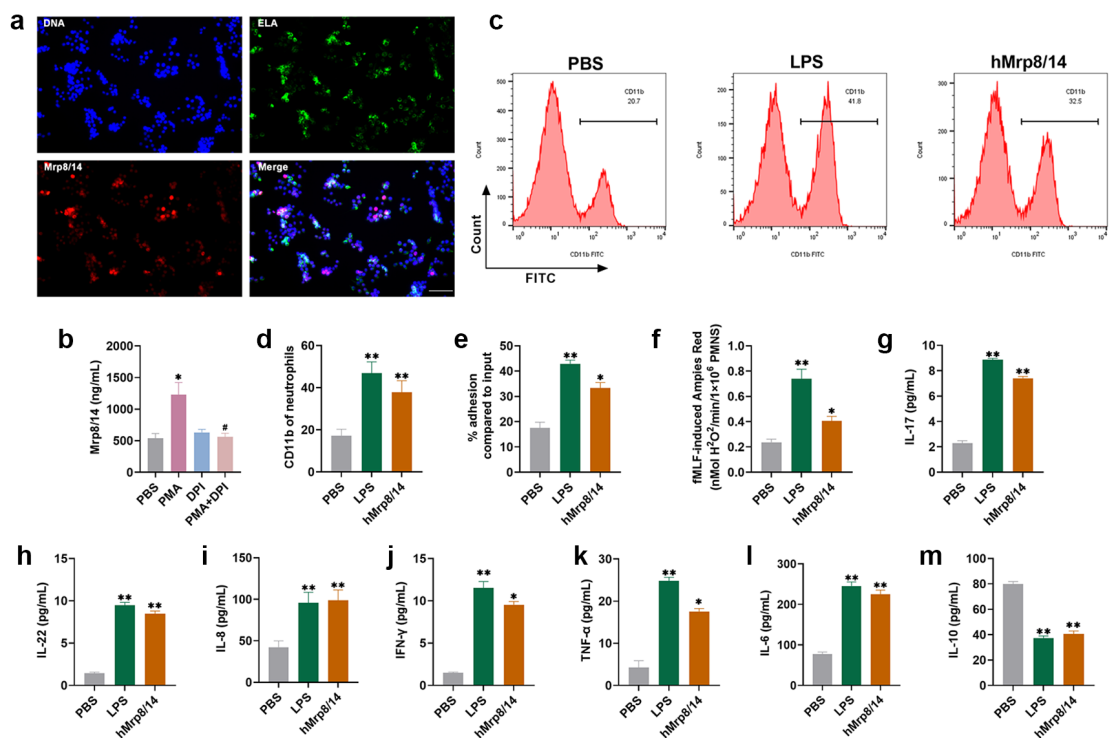


FIG. 2. Mrp8/14 release is accompanied by NETs formation and neutrophil activation.

(a) Hoechst, ELA and Mrp8/14 staining showed that PMA stimulation of neutrophils resulted in Mrp8/14 release ($40 \times$, bar = 50 μ m). (b) ELISA kit assay results confirmed that PMA treatment elevated Mrp8/14 release, whereas DPI + PMA stimulation decreased Mrp8/14 release. (c-d) Flow cytometry assays showed that both LPS and hMrp8/14 treatments increased the levels of the neutrophil activation marker CD11b. (e) Calcein AM staining results showed that both LPS and hMrp8/14 increased the percentage of adherent cells. (f) Amplex Red kit assay showed that both LPS and hMrp8/14 treatments promoted H₂O₂ release from neutrophils. (g-m) ELISA kit assay results confirmed that both LPS and hMrp8/14 treatments increased the release of IL-17, IL-22, IL-8, IFN-γ, TNF-α, and IL-6, and decreased IL-10 level. n = 3. (*p < 0.05, **p < 0.01 vs. PBS; #p < 0.05 vs. DPI). PMA, phorbol 12-myristate 13-acetate; NETs, neutrophil extracellular traps; DPI, diphenyleneiodonium; LPS, lipopolysaccharide; IL, interleukin; TNF-α, tumor necrosis factor alpha, PBS, phosphate buffer saline.

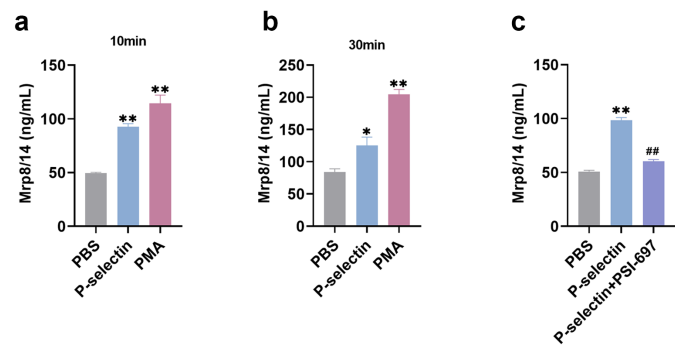


FIG. 1. The engagement of neutrophils with P-selectin causes Mrp8/14 secretion.

(a-b) ELISA kit assay showed that P-selectin treatment for 10 min or 30 min increased the level of Mrp8/14 in the supernatant of neutrophil culture, and PMA also increased the level of Mrp8/14. (c) ELISA kit assay confirmed that treatment with the P-selectin antagonist PSI-697 reduced the impact of P-selectin and decreased Mrp8/14 release. n = 3. (*p < 0.05, **p < 0.01 vs. PBS; ##p < 0.01 vs. P-selectin). PBS, phosphate buffer saline; PMA, phorbol 12-myristate 13-acetate; PSI, pneumonia severity index; Min., Minutes.

MRP8/14 activates ERK1/2-p90RSK pathway by TLR4

Numerous studies have demonstrated that MRP8/14 can interact with TLR4 to trigger neutrophil recruitment, thereby promoting various inflammatory responses.^{16,35} Our previous research revealed that MRP8/14 triggers the TLR4/NF-κB pathway in neutrophils.¹² In addition, research has shown that TLR4 mediates ERK1/2 pathway activation.³⁶ Considering the significance of the ERK1/2-p90RSK pathway in AS development³⁷, we investigated the impact of MRP8/14 on this pathway. Western blotting results demonstrated that hMRP8/14 significantly upregulated TLR4 expression and increased phosphorylation of ERK1/2 and p90RSK in neutrophils. Conversely, treatment with paquinimod, an antagonist of MRP8/14, reduced these effects, inhibiting TLR4 expression and ERK1/2-p90RSK signaling pathway activation (Figures 3a, b, Supplementary Table 2). The above results imply that MRP8/14 activates TLR4 and ERK1/2-p90RSK signaling pathways in neutrophils.

Phosphorylation of p90RSK mediates ERK5 S496 phosphorylation and inhibits the NRF2-ARE signaling pathway

Studies have shown that p90RSK phosphorylation mediates ERK5 S496 phosphorylation and blocks the Nrf2-ARE signaling pathway.²⁰ Notably, activation of the Nrf2-ARE pathway inhibits AS progression.³⁸ Therefore, we investigated how MRP8/14-mediated phosphorylation of p90RSK affects the NRF2-ARE signaling pathway. Neutrophils were first incubated with hMRP8/14 for 30 min, followed by 4 h of treatment with the p90RSK inhibitor FMK-MEA, the p90RSK agonist Ceramide C6, the ERK5-specific inhibitor AX15836, or the ERK5 agonist EGF. FMK-MEA and AX15836 treatments significantly decreased the phosphorylation level of ERK5 S496 compared to incubation with hMRP8/14 alone, while ceramide C6 and EGF significantly increased the phosphorylation level of ERK5 S496 (Figures 4a, b). This suggests that the MRP8/14-mediated phosphorylation of p90RSK facilitated the phosphorylation of ERK5 S496. In addition, FMK-MEA and AX15836 treatment caused a significant increase in Nrf2, HO-1, and NQO1 levels, while ceramide C6 and EGF treatment notably lowered these protein levels (Figures 4c, d, Supplementary Table 3). These

results verified that p90RSK phosphorylation promotes ERK5 S496 phosphorylation, thereby blocking the Nrf2-ARE signaling pathway, which may be a key mechanism by which MRP8/14 promotes AS progression.

Suppressing the NRF2-ARE signaling pathway activates neutrophils and promotes NET formation

To determine whether MRP8/14 induces neutrophil activation and NETs formation by suppressing the NRF2-ARE pathway, we studied the effects of the NRF2 inhibitor ML385 and the NRF2 agonist CDDO-Me on MRP8/14 action. Nrf2, HO-1, and NQO1 levels were markedly decreased in neutrophils after incubation with hMRP8/14 + ML385, whereas hMRP8/14 + CDDO-Me treatment markedly upregulated these proteins (Figures 5a, b). The localization of the NETs formation marker CitH3 and the neutrophil marker MPO was assessed using immunofluorescence staining. The findings indicated that hMRP8/14 + ML385 treatment notably increased the CitH3 levels in neutrophils, whereas hMRP8/14 + CDDO-Me treatment significantly reduced the fluorescence intensity of CitH3, suggesting that NRF2-ARE pathway inhibition induces NET formation (Figures 5c, d). The

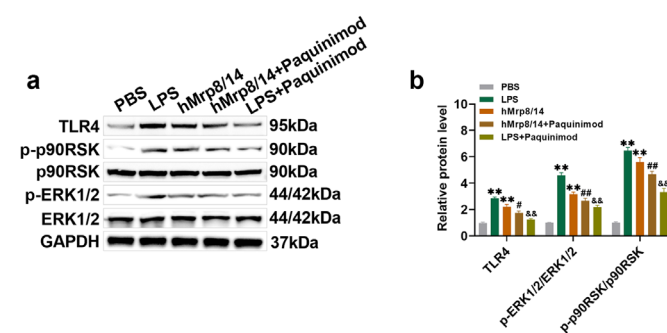


FIG. 3. Mrp8/14 activates the ERK1/2-p90RSK pathway through TLR4. (a-b) Western blot measured that both LPS and hMrp8/14 treatments increased TLR4, p-ERK1/2/ERK1/2 and p-p90RSK/p90RSK levels, while paquinimod attenuated the effect of hMrp8/14. n = 3. (*p < 0.01 vs. PBS; #p < 0.05, ##p < 0.01 vs. hMrp8/14; &&p < 0.01 vs. hMrp8/14 + paquinimod). TLR4, toll-like receptor 4; PBS, phosphate buffer saline; LPS, lipopolysaccharide; hMrp8/14, human recombinant MRP8/14.

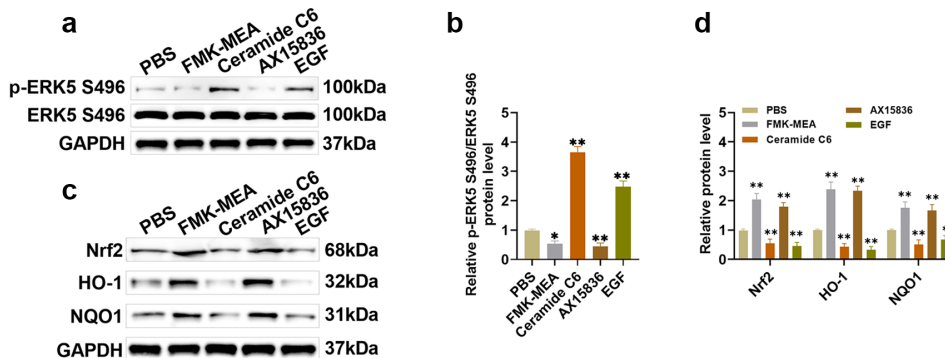


FIG. 4. Phosphorylation of p90RSK mediates ERK5 S496 phosphorylation and inhibits the NRF2-ARE signaling pathway.

(a-b) Western blot measured that both the p90RSK inhibitor FMK-MEA and the ERK5-specific inhibitor AX15836 decreased the phosphorylation level of ERK5 S496, whereas the p90RSK agonist Ceramide C6 and the ERK5 agonist EGF promoted the phosphorylation of ERK5 S496. (c-d) Western blot measured that both FMK-MEA and ERK5 increased Nrf2, HO-1, and NQO1 levels, while Ceramide C6 and EGF decreased the expression of these proteins. n=3. (*p < 0.05, **p < 0.01 vs. PBS). PBS, phosphate buffer saline.

hMRP8/14 + ML385 treatment notably increased CD11b-positive cell numbers in neutrophils, whereas the hMRP8/14 + CDDO-Me treatment decreased CD11b-positive cell numbers, suggesting that inhibition of the NRF2-ARE signaling pathway enhances neutrophil activation (Figures 5e, f). The hMRP8/14 + ML385 treatment augmented neutrophil adhesion and induced H₂O₂ release, while the hMRP8/14 + CDDO-Me treatment demonstrated the opposite effect, further confirming that inhibition of the NRF2-ARE signaling pathway induced neutrophil activation (Figures 5g, h). In addition, hMRP8/14 + ML385 treatment markedly increased IL-17, IL-22, TNF- α , IL-8, IL-6, and IFN- γ levels, while markedly decreasing IL-10 levels in the neutrophil supernatant. Conversely, hMRP8/14 + CDDO-Me treatment produced the opposite effects (Figures 5i-o, Supplementary Table 4). These results demonstrated that the NRF2 inhibitor ML385 potentiated the effect of hMRP8/14, further promoting NET formation and neutrophil activation, whereas the NRF2 agonist CDDO-Me attenuated the effect of hMRP8/14. This

suggests that MRP8/14 induces neutrophil activation and NET formation by inhibiting the NRF2-ARE pathway.

Neutrophil MRP8/14 release promotes arterial plaque formation in ApoE-/- mice in vivo

Finally, an AS mouse model was established to explore the *in vivo* effects of MRP8/14 secretion on AS progression. Oil red O staining revealed that after 12 weeks of HFD feeding, mouse aortic tissues formed distinct plaques, confirming the successful establishment of the AS mouse model; however, paquinimod treatment inhibited plaque formation (Figure 6a). Furthermore, plasma levels of TC, TG, LDL-C, and HDL-C were significantly elevated in the HFD group of mice, whereas paquinimod treatment markedly reduced these indices (Figures 6b-e). CitH3 expression levels were notably elevated in the HFD group, indicating NET formation in the aortic tissues of AS mice, whereas paquinimod treatment inhibited the NET formation (Figures 6f, g). The HFD group exhibited a significant increase in

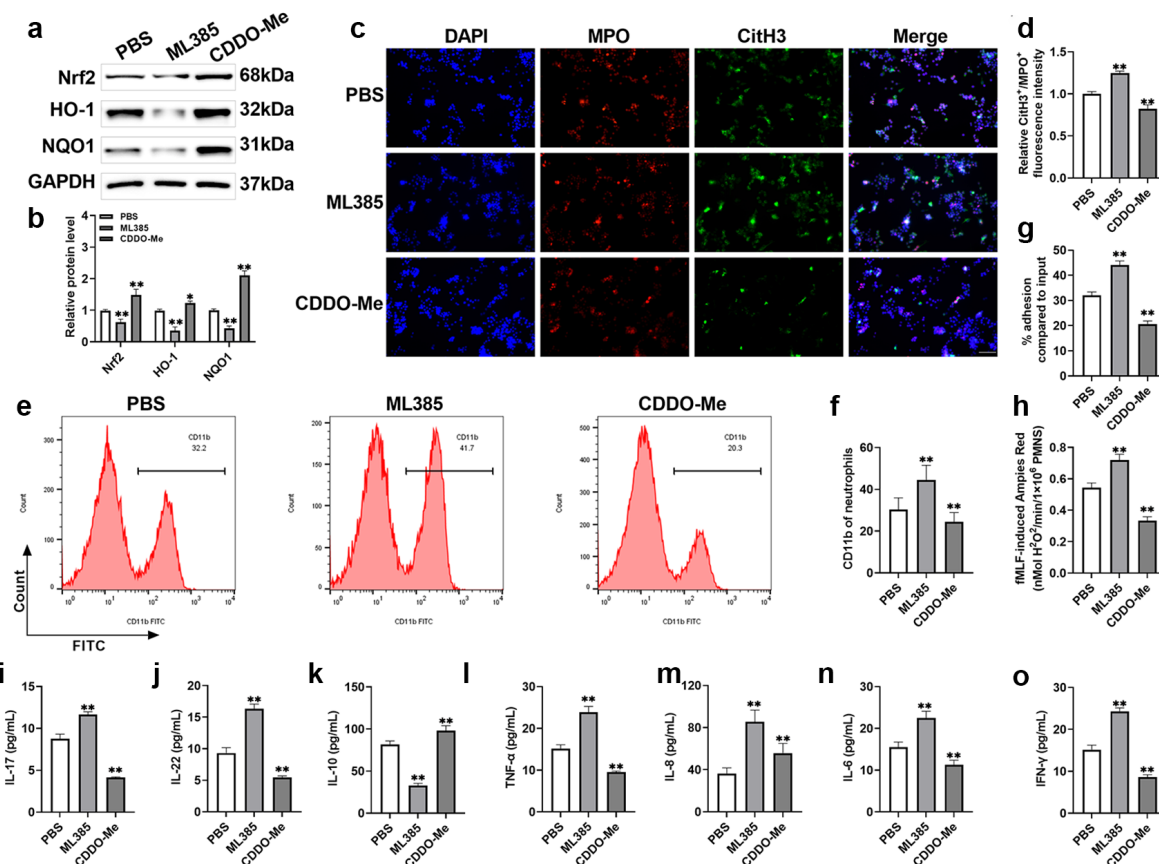


FIG. 5. Inhibition of the NRF2-ARE signaling pathway induces neutrophil activation and enhances NETs formation.

(a-b) Western blot measured that the NRF2 inhibitor ML385 decreased the NRF2-ARE pathway-related protein levels, and the NRF2 agonist CDDO-Me increased the expression of these proteins. (c-d) Immunofluorescence results confirmed that ML385 increased CitH3 expression and promoted NETs formation, while CDDO-Me did the opposite (40 \times , bar = 50 μ m). (e-f) Flow cytometry results confirmed that ML385 increased CD11b-labeled cell numbers and induced neutrophil activation, but CDDO-Me treatment caused a decline in CD11b-labeled cell numbers. (g-h) ML385 caused a rise in the number of neutrophil-adherent cells and the release of H₂O₂, while CDDO-Me led to the opposite result. (i-o) Levels of IL-17, IL-22, TNF- α , IL-6, IFN- γ , IL-8, and IL-10 in neutrophil supernatants were measured by ELISA kits. n = 3. (**p < 0.01 vs. PBS). PBS, phosphate buffer saline; NETs, neutrophil extracellular traps; IL, interleukin; TNF- α , tumor necrosis factor alpha.

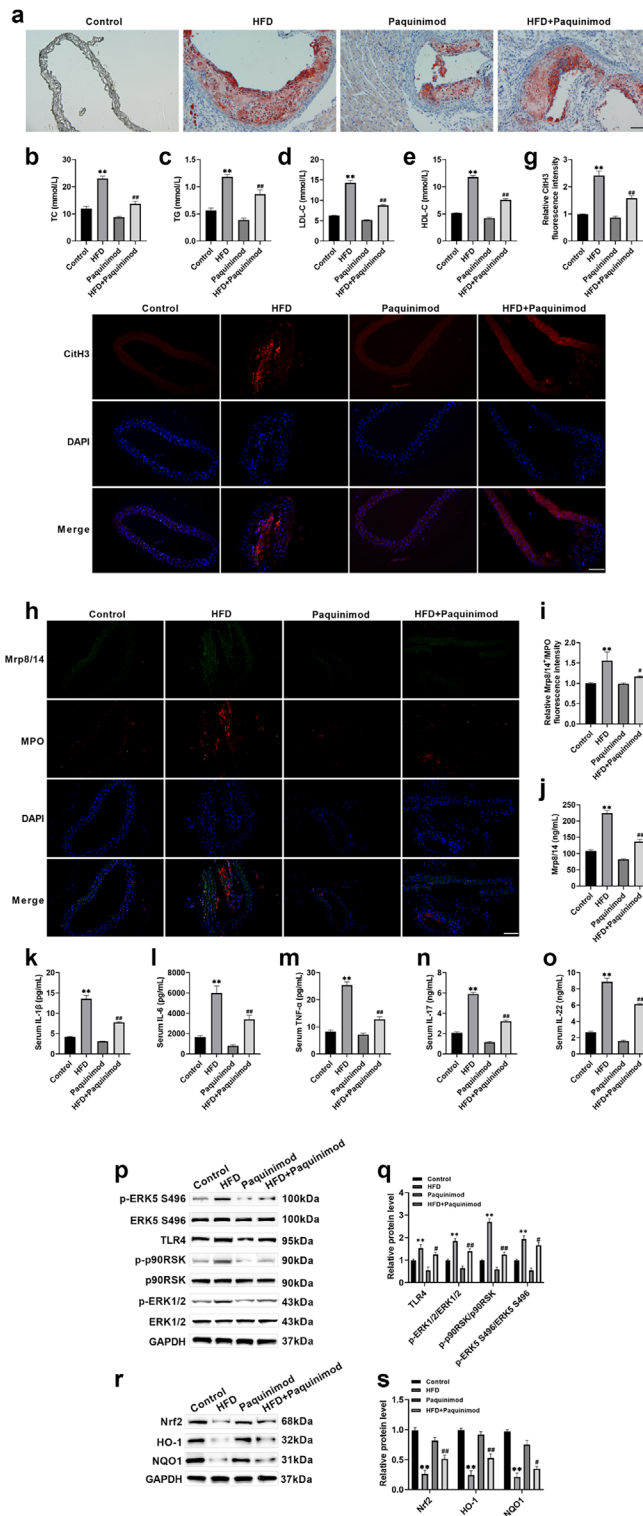


FIG. 6. Neutrophil Mrp8/14 release promotes arterial plaque formation in ApoE-/- mice in vivo.

(a) Oil red O staining determined the formation of AS plaques in mice ($20\times$, bar = 100 μ m). (b-e) TC, TG, LDL-C and HDL-C levels in plasma were assessed by different ELISA kits. (f-g) Immunofluorescence detection of CitH3 expression confirmed that HFD increased CitH3 levels and paquinimod decreased them ($20\times$, bar = 100 μ m). (h-i) Double immunofluorescence assay for the localization of Mrp8/14 and MPO confirmed that HFD promoted the release of Mrp8/14 from neutrophils in mouse aortic tissues, and paquinimod inhibited the release of Mrp8/14 ($20\times$, bar = 100 μ m). (j-o) The levels of Mrp8/14, IL-17, IL-22, IL-18, TNF- α and IL-6 in mouse serum were examined by different ELISA kits. (p-s) Western blot measured that HFD increased TLR4, p-ERK1/2/ERK1/2, p-p90RSK/p90RSK, and p-ERK5 S496/ERK5 S496 levels in mouse aortic tissues, and decreased Nrf2, HO-1, and NQO1 levels, and paquinimod reversed HFD's effect. n = 6. (**p < 0.01 vs. control; #p < 0.05, ##p < 0.01 vs. HFD). TC, total cholesterol; TG, triglyceride; LDL-C, low density lipoprotein cholesterol; HDL-C, high density lipoprotein cholesterol; CitH3, citrullinated histone h3; HFD, high fat diet; IL, interleukin.

MRP8/14 fluorescence intensity, indicating substantial release of MRP8/14 from neutrophils in AS mice; this effect was attenuated by paquinimod treatment (Figures 6h, i). The serum levels of MRP8/14, IL-17, IL-22, IL-1 β , TNF- α , and IL-6 were significantly raised in the HFD group, whereas paquinimod treatment markedly mitigated proinflammatory cytokine levels (Figures 6j-o). The TLR4 protein and the phosphorylation levels of ERK1/2, p90RSK, and ERK5 S496 were markedly elevated, whereas Nrf2, HO-1, and NQO1 levels were notably downregulated in the HFD group. These alterations were reversed following paquinimod treatment (Figures 6p-s, Supplementary Table 5). These results indicate that aortic tissue neutrophils of AS mice secreted MRP8/14, which in turn induced NET formation and neutrophil activation, activated the ERK1/2-p90RSK pathway, and blocked the NRF2-ARE pathway, thereby inducing inflammatory responses. In contrast, inhibition of MRP8/14 secretion mitigated the inflammatory response in aortic tissues of AS mice.

DISCUSSION

According to previous studies, arterial endothelial cell dysfunction results in abnormally elevated expression of adhesion molecules, increased adhesion of circulating leukocytes and platelets, excessive release of inflammatory factors, chemokines, etc. LDL undergoes oxidation to form oxidized-LDL (ox-LDL), which is then engulfed by macrophages, causing the formation of foam cells. Concurrently, the excessive proliferation of smooth muscle cells contributes to vascular remodeling, ultimately leading to the development of AS.³⁹⁻⁴¹ Neutrophils represent the largest population of leukocytes found in the circulation and are essential for both innate and adaptive immune responses.⁴² Neutrophil recruitment is regulated by chemokines and intercellular adhesion molecules, and P-selectin facilitates neutrophil adhesion to vascular endothelial cells, thereby inducing an inflammatory response in the vascular wall. Elevated P-selectin levels accelerate AS progression.^{32,33} In a previous study, we discovered that P-selectin on platelets interacts with P-selectin glycoprotein ligand-1 on neutrophils, thereby promoting MRP8/14 secretion.¹² This study found that the P-selectin antagonist PSI-697 decreased MRP8/14 secretion, further verifying that P-selectin interacts with neutrophils to induce MRP8/14 release. Additionally, MRP8/14 levels were elevated in the aortic tissues of the HFD-induced AS mouse model, implying that MRP8/14 is involved in AS progression. Notably, treatment with the MRP8/14 antagonist paquinimod inhibited AS plaque formation, confirming the critical role of MRP8/14 release in AS progression.

During inflammation and infection of the organism, neutrophils migrate from the periphery to the corresponding tissues to enhance host defense and facilitate the immune response. This process is accompanied by phagocytosis as well as ROS and NET production.⁴³ NETs comprise extracellular structures composed of cytoplasmic proteins, decondensed neutrophil chromatin, and granules.⁴⁴ NETs are an important component of the immune response, eliminating pathogens such as fungi, bacteria, viruses, and parasites.⁴⁵ However, NETs serve a dual purpose; while they contribute to host defense, they can also aid in the generation and release of autoantigens,

potentially promoting the onset and progression of inflammatory conditions.⁴⁶ Josefs et al.⁴⁷ discovered that the NETs promote proinflammatory macrophage activation and AS plaque formation in mice. Sano et al.⁴⁸ demonstrated that induction of NET formation inhibits autophagosome formation in macrophages, whereas the inhibition of NET formation decreases the area of AS lesions in mice. In our research, inhibition of NET formation significantly reduced MRP8/14 release from neutrophils, implying that MRP8/14 release is accompanied by NET formation. Schenten et al.³⁰ also discovered that MRP8/14 release in neutrophils correlates with NET formation and that MRP8/14 and NETs can co-localize. Additionally, treatment of neutrophils with hMRP8/14 significantly promoted their activation and triggering, increased their adhesion, and thereby induced substantial secretion of proinflammatory factors and chemokines, suggesting that MRP8/14 may be a significant contributor to AS progression.

TLR4, the most widely studied receptor in the TLR family, is vital in lipid metabolism disorders, chronic inflammatory responses, and immune responses.⁴⁹ Numerous studies have validated that TLR4 is crucial for several pathological processes in AS development, predominantly involving inflammation, cholesterol metabolism, plaque stability, and vascular remodeling.^{19,50} In addition, TLR4 recognizes LPS, and its binding induces intracellular transcription of inflammatory mediators whose inflammatory response has been implicated in AS development.⁵¹ Yonekawa et al.⁵² demonstrated that MRP8/14 binds to TLR4 and promotes inflammatory cytokine secretion from monocytes involved in the progression of acute coronary syndromes. Similarly, our research discovered that hMRP8/14 treatment upregulated TLR4 expression in neutrophils. It has been reported that the MRP8/14 antagonist paquinimod not only inhibits MRP8/14 release but also the binding of MRP8/14 to TLR4.⁵³ In this study, paquinimod treatment attenuated the effect of hMRP8/14 and downregulated TLR4 expression, consistent with previously reported findings. In addition, oral administration of paquinimod downregulated TLR4 expression in the aortic tissues of AS mice, further confirming that MRP8/14 can bind to TLR4.

TLR4 activates the ERK1/2 pathway and induces p90RSK phosphorylation.^{36,54} Research indicated that blocking the ERK1/2-p90RSK pathway decreases the migration and proliferation of rat aortic smooth muscle cells, which are crucial in AS progression.³⁷ The NRF2-ARE pathway plays a pivotal role in the cellular oxidative stress response and is regarded as a key antioxidant mechanism, as it reduces both endogenous and exogenous oxidative and chemical-induced oxidative stress responses.^{55,56} When the NRF2-ARE signaling pathway is activated, it impedes the proliferation and migration of vascular smooth muscle cells, whereas NRF2 deficiency accelerates AS progression in mice.^{57,58} In this study, hMRP8/14 treatment elevated ERK1/2 and p90RSK phosphorylation levels, whereas Paquinimod mitigated the effect of hMRP8/14 treatment. In addition, both p90RSK and ERK5 agonists increased the phosphorylation level of ERK5 S496 and inhibited the Nrf2-ARE pathway activation, suggesting that MRP8/14-mediated phosphorylation of p90RSK promotes ERK5 S496 phosphorylation and blocks the Nrf2-ARE pathway, which is consistent with the results reported by Singh et al.²⁰ Notably, inhibition of the NRF2-ARE signaling pathway facilitates neutrophil

activation, promotes NET formation, and induces an inflammatory response. Activation of the ERK1/2-p90RSK pathway and blockade of the NRF2-ARE signaling pathway were also noted in the aortic tissues of AS mice. The inhibition of MRP8/14 release augmented inflammatory responses, blocked the ERK1/2-p90RSK pathway, and activated the NRF2-ARE signaling pathway, suggesting that MRP8/14 may play a critical role in AS progression by regulating the ERK1/2-p90RSK/NRF2-ARE pathway.

In summary, platelet-neutrophil interaction-derived MRP8/14 promotes neutrophil activation and modulates the ERK1/2-p90RSK/NRF2-ARE signaling pathway via TLR4, inducing neutrophils to secrete proinflammatory factors, which may be a key mechanism for AS progression. This study elucidated the underlying mechanism of MRP8/14-induced inflammation, demonstrated that MRP8/14 may serve as a potential target for AS treatment, and enriched the therapeutic approach for AS. Unfortunately, the physiological milieu of the human body is extremely complex. Factors such as the inter-cell interaction, hormone levels, and the overall regulation of the immune system are difficult to fully reproduce *in vitro*. This study provides a preliminary theoretical basis for the potential role and mechanism of MRP8/14 in AS. In the future, genetic models such as A-related gene knockout mice need to be employed to further validate the association between MRP8/14 signal transduction and AS progression. In addition, due to limited experimental conditions, the sample size in this study was minimal and should be further expanded in the future to enhance the reliability and generalizability of the findings.

Ethics Committee Approval: Approval for the animal research was obtained from the Animal Ethics and Welfare Committee.

Informed Consent: Patient consent information is not required.

Data Sharing Statement: The datasets analyzed during the current study are available from the corresponding author upon reasonable request.

Authorship Contributions: Data Collection or Processing- X.L., L.W.; Analysis or Interpretation- X.Li; Writing- J.L., L.W.; Critical Review- L.W.

Conflict of Interest: The authors declare that they have no conflict of interest.

Funding: The Fundamental Research Funds for the Provincial Universities (no: 2024).

Supplementary: <https://www.balkanmedicaljournal.org/img/files/balkan-2025-4-73-supplement.pdf>

REREFENCES

- Kong P, Cui ZY, Huang XF, Zhang DD, Guo RJ, Han M. Inflammation and atherosclerosis: signaling pathways and therapeutic intervention. *Signal Transduct Target Ther.* 2022;7:131. [\[CrossRef\]](#)
- Pedro-Botet J, Climent E, Benaiges D. Atherosclerosis and inflammation. New therapeutic approaches. *Med Clin (Barc).* 2020;155:256-262. [\[CrossRef\]](#)
- Libby P, Buring JE, Badimon L, et al. Atherosclerosis. *Nat Rev Dis Primers.* 2019;5:56. [\[CrossRef\]](#)
- Ruiz-León AM, Lapuente M, Estruch R, Casas R. Clinical advances in immunonutrition and atherosclerosis: a review. *Front Immunol.* 2019;10:837. [\[CrossRef\]](#)
- GBD 2019 Peripheral Artery Disease Collaborators. Global burden of peripheral artery disease and its risk factors, 1990-2019: a systematic analysis for the Global Burden of Disease Study 2019. *Lancet Glob Health.* 2023;11:e1553-e1565. [\[CrossRef\]](#)
- Chen W, Li Z, Zhao Y, Chen Y, Huang R. Global and national burden of atherosclerosis from 1990 to 2019: trend analysis based on the Global Burden of Disease Study 2019. *Chin Med J (Engl).* 2023;136:2442-2450. [\[CrossRef\]](#)
- Chen X, Giles J, Yao Y, et al. The path to healthy ageing in China: a Peking University-Lancet Commission. *Lancet.* 2022;400:1967-2006. [\[CrossRef\]](#)
- Fan J, Watanabe T. Atherosclerosis: known and unknown. *Pathol Int.* 2022;72:151-160. [\[CrossRef\]](#)
- Libby P. Inflammation and the pathogenesis of atherosclerosis. *Vascul Pharmacol.* 2024;154:107255. [\[CrossRef\]](#)
- Blagov AV, Markin AM, Bogatyreva AI, Tolstik TV, Sukhorukov VN, Orekhov AN. The Role of Macrophages in the Pathogenesis of Atherosclerosis. *Cells.* 2023;12:522. [\[CrossRef\]](#)
- Döring Y, van der Vorst EPC, Weber C. Targeting immune cell recruitment in atherosclerosis. *Nat Rev Cardiol.* 2024;21:824-840. [\[CrossRef\]](#)
- Liang X, Xiu C, Liu M, et al. Platelet-neutrophil interaction aggravates vascular inflammation and promotes the progression of atherosclerosis by activating the TLR4/NF-κB pathway. *J Cell Biochem.* 2019;120:5612-5619. [\[CrossRef\]](#)
- Meng LB, Yu ZM, Guo P, et al. Neutrophils and neutrophil-lymphocyte ratio: Inflammatory markers associated with intimal-media thickness of atherosclerosis. *Thromb Res.* 2018;170:45-52. [\[CrossRef\]](#)
- Wang J, Chen G, Li L, et al. Sustained induction of IP-10 by MRP8/14 via the IFN-β-IRF7 axis in macrophages exaggerates lung injury in endotoxemic mice. *Burns Trauma.* 2023;11:tkad006. [\[CrossRef\]](#)
- Foell D, Saers M, Park C, et al. A novel serum calprotectin (MRP8/14) particle-enhanced immuno-turbidimetric assay (sCAL turbo) helps to differentiate systemic juvenile idiopathic arthritis from other diseases in routine clinical laboratory settings. *Mol Cell Pediatr.* 2023;10:14. [\[CrossRef\]](#)
- Revenstorff J, Ludwig N, Hilger A, et al. Role of S100A8/A9 in platelet-neutrophil complex formation during acute inflammation. *Cells.* 2022;11:3944. [\[CrossRef\]](#)
- An Z, Li J, Yu J, Wang X, et al. Neutrophil extracellular traps induced by IL-8 aggravate atherosclerosis via activation NF-κB signaling in macrophages. *Cell cycle (Georgetown, Tex).* 2019;18:2928-2938. [\[CrossRef\]](#)
- Bagheri B, Khatibiyani Feyzabadi Z, Nouri A, et al. Atherosclerosis and Toll-like receptor4 (TLR4), lectin-like oxidized low-density lipoprotein-1 (LOX-1), and proprotein convertase subtilisin/kexin type9 (PCSK9). *Mediators Inflamm.* 2024;2024:5830491. [\[CrossRef\]](#)
- Li Y, Zhang L, Ren P, et al. Qing-Xue-Xiao-Zhi formula attenuates atherosclerosis by inhibiting macrophage lipid accumulation and inflammatory response via TLR4/MyD88/NF-κB pathway regulation. *Phytomedicine.* 2021;93:153812. [\[CrossRef\]](#)
- Singh MV, Kotla S, Le NT, et al. Senescent phenotype induced by p90RSK-NRF2 signaling sensitizes monocytes and macrophages to oxidative stress in HIV-positive individuals. *Circulation.* 2019;139:1199-1216. [\[CrossRef\]](#)
- Chen X, Duong MN, Nicholls SJ, Bursill C. Myeloperoxidase modification of high-density lipoprotein suppresses human endothelial cell proliferation and migration via inhibition of ERK1/2 and Akt activation. *Atherosclerosis.* 2018;273:75-83. [\[CrossRef\]](#)
- Xia S, Menden HL, Korfhagen TR, Kume T, Sampath V. Endothelial immune activation programmes cell-fate decisions and angiogenesis by inducing angiogenesis regulator DLL4 through TLR4-ERK-FOXC2 signalling. *J Physiol.* 2018;596:1397-1417. [\[CrossRef\]](#)
- Wang C, Wang S, Ma X, et al. P-selectin facilitates SARS-CoV-2 spike 1 subunit attachment to vesicular endothelium and platelets. *ACS Infect Dis.* 2024;10:2656-2667. [\[CrossRef\]](#)
- Abe RJ, Savage H, Imanishi M, et al. p90RSK-MAGI1 module controls endothelial permeability by post-translational modifications of MAGI1 and hippo pathway. *Front Cardiovasc Med.* 2020;7:542485. [\[CrossRef\]](#)
- Lee Y, Na J, Lee MS, et al. Combination of pristimerin and paclitaxel additively induces autophagy in human breast cancer cells via ERK1/2 regulation. *Mol Med Rep.* 2018;18:4281-4288. [\[CrossRef\]](#)
- Abe JL, Imanishi M, Li S, et al. An ERK5-NRF2 axis mediates senescence-associated stemness and atherosclerosis. *Circ Res.* 2023;133:25-44. [\[CrossRef\]](#)
- Erazo T, Espinosa-Gil S, Diéguez-Martínez N, Gómez N, Lizcano JM. SUMOylation Is required for ERK5 nuclear translocation and ERK5-mediated cancer cell proliferation. *Int J Mol Sci.* 2020;21:2203. [\[CrossRef\]](#)
- Wang Z, Yao M, Jiang L, et al. Dexmedetomidine attenuates myocardial ischemia/reperfusion-induced ferroptosis via AMPK/GSK-3β/Nrf2 axis. *Biomed Pharmacother.* 2022;154:113572. [\[CrossRef\]](#)

29. Amirova KM, Dimitrova PA, Leseva MN, Koycheva IK, Dinkova-Kostova AT, Georgiev MI. The triterpenoid Nrf2 activator, CDDO-me, decreases neutrophil senescence in a murine model of joint damage. *Int J Mol Sci.* 2023;24:8775. [\[CrossRef\]](#)
30. Schenten V, Plançon S, Jung N, et al. Secretion of the phosphorylated form of S100A9 from neutrophils is essential for the proinflammatory functions of extracellular. *Front Immunol.* 2018;9:447. [\[CrossRef\]](#)
31. Sprenkeler EGG, Zandstra J, van Kleef N, et al. S100A8/A9 Is a marker for the release of neutrophil extracellular traps and induces neutrophil activation. *Cells.* 2022;11:236. [\[CrossRef\]](#)
32. Zinelli A, Mangoni AA. Systematic review and meta-analysis of the effect of statins on circulating e-selectin, l-selectin, and p-selectin. *Biomedicines.* 2021;9:1707. [\[CrossRef\]](#)
33. Sommer P, Schreinlechner M, Noflatscher M, et al. Increasing soluble p-selectin levels predict higher peripheral atherosclerotic plaque progression. *J Clin Med.* 2023;12:6430. [\[CrossRef\]](#)
34. Miralda I, Uriarte SM, McLeish KR. Multiple phenotypic changes define neutrophil priming. *Front Cell Infect Microbiol.* 2017;7:217. [\[CrossRef\]](#)
35. Pruenster M, Vogl T, Roth J, Sperandio M. S100A8/A9: from basic science to clinical application. *Pharmacol Ther.* 2016;167:120-131. [\[CrossRef\]](#)
36. Blair L, Pattison MJ, Chakravarty P, et al. TPL-2 Inhibits IFN- β expression via an ERK1/2-TCF-FOS axis in TLR4-stimulated macrophages. *J Immunol.* 2022;208:941-954. [\[CrossRef\]](#)
37. Huynh DTN, Jin Y, Van Nguyen D, Myung CS, Heo KS. Ginsenoside Rh1 inhibits angiotensin II-induced vascular smooth muscle cell migration and proliferation through suppression of the ROS-mediated ERK1/2/p90RSK/KLF4 signaling pathway. *Antioxidants (Basel).* 2022;11:643. [\[CrossRef\]](#)
38. Gu L, Ye P, Li H, et al. Lunasin attenuates oxidant-induced endothelial injury and inhibits atherosclerotic plaque progression in ApoE-/- mice by up-regulating heme oxygenase-1 via PI3K/Akt/Nrf2/ARE pathway. *FASEB J.* 2019;33:4836-4850. [\[CrossRef\]](#)
39. Khatana C, Saini NK, Chakrabarti S, et al. Mechanistic insights into the oxidized Low-density lipoprotein-induced atherosclerosis. *Oxid Med Cell Longev.* 2020;2020:5245308. [\[CrossRef\]](#)
40. He Y, Liu T. Oxidized low-density lipoprotein regulates macrophage polarization in atherosclerosis. *Int Immunopharmacol.* 2023;120:110338. [\[CrossRef\]](#)
41. Malekmohammad K, Sewell RDE, Rafieian-Kopaei M. Antioxidants and atherosclerosis: mechanistic aspects. *Biomolecules.* 2019;9:301. [\[CrossRef\]](#)
42. Liew PX, Kubis P. The Neutrophil's Role During Health and Disease. *Physiol Rev.* 2019;99:1223-1248. [\[CrossRef\]](#)
43. Metzemaekers M, Gouwy M, Proost P. Neutrophil chemoattractant receptors in health and disease: double-edged swords. *Cell Mol Immunol.* 2020;17:433-450. [\[CrossRef\]](#)
44. Mutua V, Gershwin LJ. A review of neutrophil extracellular traps (NETs) in disease: potential anti-NETs therapeutics. *Clin Rev Allergy Immunol.* 2021;61:194-211. [\[CrossRef\]](#)
45. Demkow U. Molecular mechanisms of neutrophil extracellular trap (NETs) degradation. *Int J Mol Sci.* 2023;24:4896. [\[CrossRef\]](#)
46. Lee KH, Kronbichler A, Park DD, et al. Neutrophil extracellular traps (NETs) in autoimmune diseases: a comprehensive review. *Autoimmun Rev.* 2017;16:1160-1173. [\[CrossRef\]](#)
47. Josefs T, Barrett TJ, Brown EJ, et al. Neutrophil extracellular traps promote macrophage inflammation and impair atherosclerosis resolution in diabetic mice. *JCI insight.* 2020;5:e134796. [\[CrossRef\]](#)
48. Sano M, Maejima Y, Nakagama S, et al. Neutrophil extracellular traps-mediated Beclin-1 suppression aggravates atherosclerosis by inhibiting macrophage autophagy. *Front Cell Dev Biol.* 2022;10:876147. [\[CrossRef\]](#)
49. Kim HJ, Kim H, Lee JH, Hwangbo C. Toll-like receptor 4 (TLR4): new insight immune and aging. *Immun Ageing.* 2023;20:67. [\[CrossRef\]](#)
50. Quan YZ, Ma A, Ren CQ, et al. Ganoderic acids alleviate atherosclerosis by inhibiting macrophage M1 polarization via TLR4/MyD88/NF- κ B signaling pathway. *Atherosclerosis.* 2024;391:117478. [\[CrossRef\]](#)
51. Miller YI, Choi SH, Wiesner P, Bae YS. The SYK side of TLR4: signalling mechanisms in response to LPS and minimally oxidized LDL. *Br J Pharmacol.* 2012;167:990-999. [\[CrossRef\]](#)
52. Yonekawa K, Neidhart M, Altwegg LA, et al. Myeloid related proteins activate toll-like receptor 4 in human acute coronary syndromes. *Atherosclerosis.* 2011;218:486-492. [\[CrossRef\]](#)
53. Su M, Chen C, Li S, et al. Gasdermin D-dependent platelet pyroptosis exacerbates NET formation and inflammation in severe sepsis. *Nature Cardiovasc Res.* 2022;1:732-747. [\[CrossRef\]](#)
54. Wu JH, Hong LC, Tsai YY, Chen HW, Chen WX, Wu TS. Mitogen-activated protein kinase (MAPK) signalling pathways in HepG2 cells infected with a virulent strain of Klebsiella pneumoniae. *Cell Microbiol.* 2006;8:1467-1474. [\[CrossRef\]](#)
55. Liu S, Pi J, Zhang Q. Signal amplification in the KEAP1-NRF2-ARE antioxidant response pathway. *Redox Biol.* 2022;54:102389. [\[CrossRef\]](#)
56. Li B, Wang Y, Jiang X, et al. Natural products targeting Nrf2/ARE signaling pathway in the treatment of inflammatory bowel disease. *Biomed Pharmacother.* 2023;164:114950. [\[CrossRef\]](#)
57. Barajas B, Che N, Yin F, et al. NF-E2-related factor 2 promotes atherosclerosis by effects on plasma lipoproteins and cholesterol transport that overshadow antioxidant protection. *Arterioscler Thromb Vasc Biol.* 2011;31:58-66. [\[CrossRef\]](#)
58. Jiang H, Zhao Y, Feng P, Liu Y. Sulfiredoxin-1 inhibits PDGF-BB-induced vascular smooth muscle cell proliferation and migration by enhancing the activation of Nrf2/ ARE signaling. *Int Heart J.* 2022;63:113-121. [\[CrossRef\]](#)